IAHR AIRH
39th IAHR
WORLD CONGRESS
GRANADA, SPAIN 2022
From Snow to Sea
19-24 June 2022
Hosted by Spain Water and IWHR, China

Proceedings of the 39th IAHR World Congress
19-24 June 2022
Granada, Spain
DOI number

Overtopping-Induced Failure of Non–Cohesive Homogeneous Fluvial Dikes: Effect of Dike Geometry on Breach Discharge

Vincent Schmitz(1), Sébastien Erpicum(1), Ismail Rifai(2), Kamal El Kadi Abderrezzak(3) (4), Pierre Archambeau(1), Michel Pirotton(1) and Benjamin Dewals(1)

(1) Research Group of Hydraulics in Environmental and Civil Engineering (HECE), University of Liège, Liège, Belgium
V.Schmitz@uliege.be

(2) Egis, Guyancourt, France

(3) National Laboratory for Hydraulics and Environment (LNHE), EDF R&D, Chatou, France

(4) Saint Venant Laboratory for Hydraulics, Chatou, France

Abstract

Laboratory experiments were conducted to evaluate the impact of dike geometry on the breaching of non-cohesive homogeneous fluvial dikes. The influence of the dike crest length and the channel-side and floodplain-side slopes on the breach discharge time-evolution was highlighted. Dikes with a larger volume per unit width lead to a more progressive increase in breach discharge during the first stage of breach expansion (i.e., phase of rapid erosion) whilst having little influence on the latter stage of the breaching process. Two extreme configurations, i.e. dikes with particularly small and large volume per unit width, allowed us to confirm these trends. The breach hydrographs were observed to follow three distinct patterns, which are explained based on a normalized form of the dike unit volume and the Froude number in the main channel. Through the implementation of a simple conceptual model, we showed that any breach hydrograph may be seen as the combination of two systems: a dam breaching and an open-channel flow.

Keywords: Dike breaching; Overtopping; Dike geometry; Breach discharge; Breach hydrograph

1. INTRODUCTION

Fluvial dikes are crucial structures that protect floodplains along river stretches. Therefore, understanding their breaching mechanisms is of prime importance. While most previous studies focused on dam breaching, few considered fluvial dikes. Rifai et al. (2017; 2018) highlighted the influence of several parameters (e.g. main channel inflow discharge, downstream boundary conditions, floodplain tailwater) on the breaching process of non–cohesive homogeneous fluvial dikes induced by overtopping, which is the most common failure type. However, the impact of the dike geometry was never investigated systematically.

In this research, we tested eight fluvial dike configurations in laboratory to highlight the individual impact of three geometrical parameters (both side slopes of the dike and its crest width) on the breach hydrograph. For each tested configuration, three inflow discharges were used. Extreme configurations, i.e. dikes with a particularly small and large volume per unit width, were tested to confirm the observed trends. Based on main channel inlet Froude number and dike non-dimensional volume per unit width, breach hydrographs were classified according to three distinct patterns. A simple conceptual model was developed to show that any dike breach hydrograph may be interpreted as the result of a combination of a dam breaching and an open-channel flow.

2. LABORATORY EXPERIMENTS

The laboratory setup is the same as that used by Rifai et al. (2017; 2018). It consists of a horizontal, straight main channel (10 m x 1 m) with a 3-m-long lateral opening toward a floodplain (4.3 m x 2.5 m). Along the side opening, sand was gathered and compacted to build a trapezoidal shaped fluvial dike, whose dimensions were systematically varied while keeping the dike height constant (0.3 m). The dike geometry is characterized by the upstream slope S_u, the downstream slope S_d and the crest length L_k (Figure 1).

A specific coating was applied on the surfaces of the main channel and the floodplain to ensure roughness continuity between those surfaces and the dike. To reduce seepage flow, a drainage system was installed at the dike bottom. Finally, a perforated plate followed by a tank were placed at the end of the main channel to control the downstream water level and to collect the main channel outlet flow.

Each geometrical configuration was tested with three different but constant main channel inflow discharges, i.e. Q_{in} = 25 l/s, 40 l/s and 55 l/s. During the filling phase, the water level rose in the main channel. The perforated plate was calibrated such that just before breaching the water level corresponded to the dike height. Before starting the tests, a 2-cm-deep and 10-cm-wide notch was created in the crest, 0.8 m far from the upstream end of the dike, to trigger breaching at a fixed location. Once the water level overtopped the notch, erosion and breaching developed.

The water level in the main channel was recorded in three locations using ultrasonic sensors (G1, G2 and G3). Similar sensors were used to monitor the water level in the outflow tank (G4) and in the drainage tank (G5). The inflow discharge was measured using an electromagnetic flowmeter. The breach discharge was determined from mass balance considering the main channel inlet and outlet flows, storage in the main channel, as well as the drainage flow (Rifai et al., 2017).

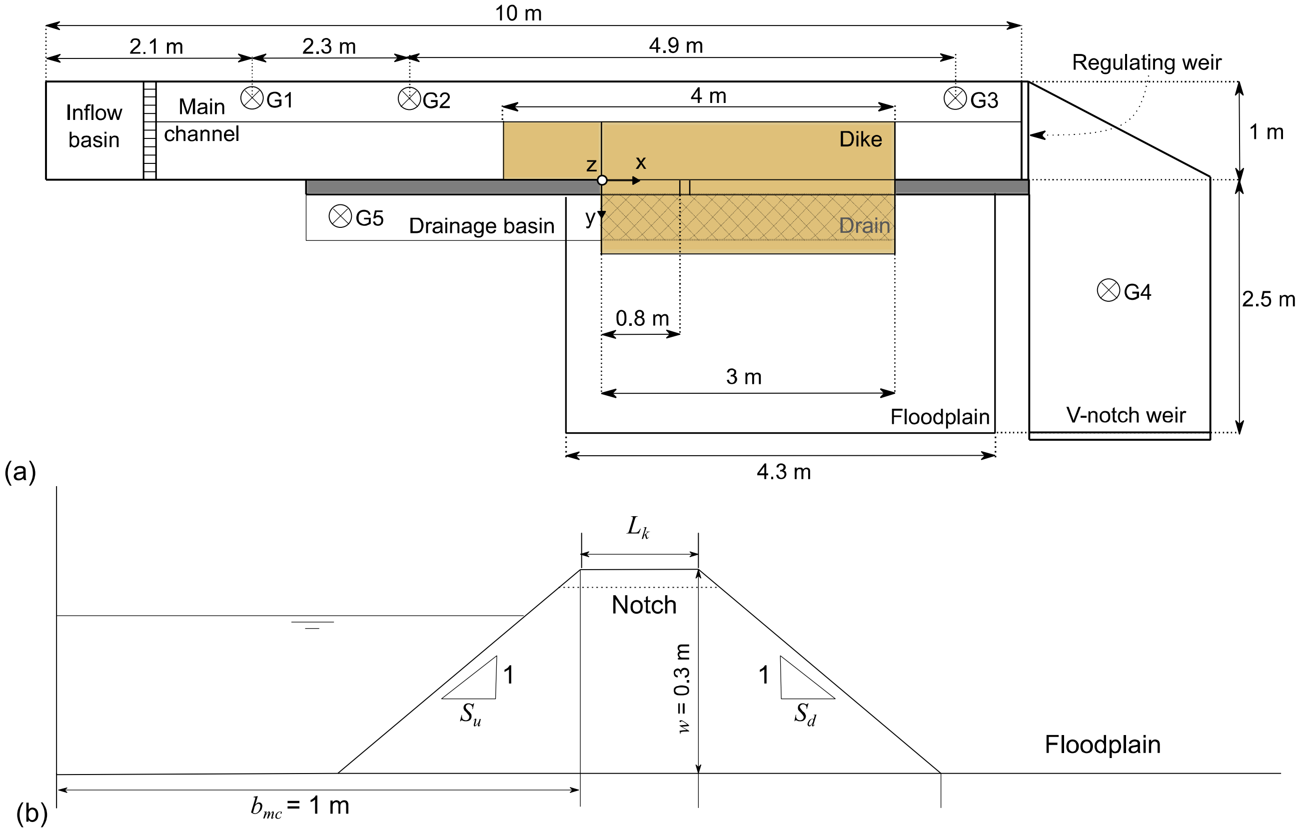

Figure 1. Experimental setup: (a) plane view; (b) dike vertical profile, highlighting main geometric parameters: channel-side and floodplain-side dike slopes (S_u and S_d), height (w) and crest length (L_k).

3. RESULTS

In line with Müller et al. (2016) for dam breaching, we used a non-dimensional parameter μ, defined as the dike volume per unit width ($L_k\, w + w^2\, (S_u + S_d) / 2$) normalized by its value for a dike of identical height w but characterized by the following non-dimensional geometric parameters: $S_u = S_d = 2$ and $L_k / w = 0.5$. This parameter adequately summarizes the impact of the dike side slopes and crest length. When increasing μ, i.e. when S_u, S_d or L_k grows, the phase of rapid erosion (Stage 1) of the breach hydrograph slows down, as shown in Figure 2. This trend becomes clearer when the inflow discharge rises. The transition between Stage 1 and Stage 2 (i.e. phase of gradual breach widening) becomes more gradual when μ increases. The impact of the dike geometry on Stage 2 is less marked and all curves tend to converge towards a quasi-equilibrium value (Michelazzo et al., 2018). Comparing Figure 2a, 2b and 2c reveals that increasing the Froude number (or alternatively the inflow discharge) in the main channel tends to make the transition between Stages 1 and 2 more gradual. Varying the Froude number alters also the overall slope of the breach hydrographs, as discussed hereafter.

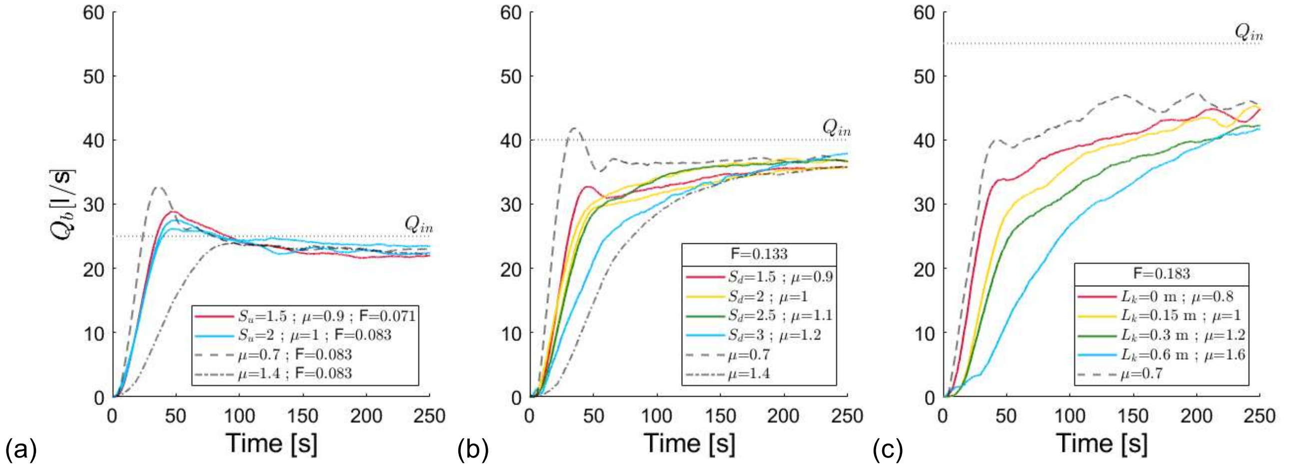

Figure 2. Examples of measured breach hydrographs: (a) effect of varying the upstream dike slope, with Q_{in} = 25 l/s; (b) effect of varying the downstream dike slope, with Q_{in} = 40 l/s; (c) effect of varying the crest length, with Q_{in} = 55 l/s. The reference configuration corresponds to S_u = S_d = 2 and L_k = 0.15 m. Grey dashed curves correspond to particularly small dikes whilst grey dash-dotted curves represent particularly large dikes.

Three distinct hydrograph patterns emerge from the laboratory observations (Figure 3). Type A hydrographs arise when μ and main channel inlet Froude number (or inflow discharge) are small. They exhibit a steep initial rise followed by a global maximum, a decline and a plateau corresponding to the equilibrium breach discharge, Q_{NE}. Type C hydrographs appear when μ and the Froude number are large. They show a continuously increasing evolution towards a quasi-equilibrium breach discharge. No maximum is observed nor clear transition between Stages 1 and 2. Finally, Type B hydrographs appear for intermediate configurations. They exhibit a local maximum, a decline and a gradual rise towards an equilibrium or quasi-equilibrium breach discharge.

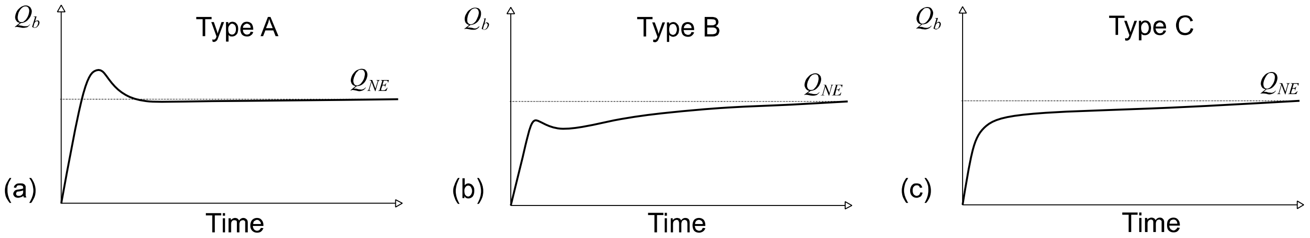

Figure 3. Breach hydrograph patterns.

Hydrograph types obtained through multiple experimental test campaigns were identified and the corresponding tests were plotted as a function of non-dimensional volume per unit width, μ, and Froude number, F (Figure 4). It shows that the classification presented in Figure 3 can be generalized to other configurations. Transition zones separate hydrograph types and approximately correspond to $F \times \mu = 0.1$, and $\mu = 0.9$ ($F \times \mu > 0.1$). Though, these zones are not clear-cut and should therefore be interpreted in a qualitative way.

Finally, we developed a simple conceptual model based on the assumption that a dike breaching event results from the combination of two extreme configurations: the failure of an embankment dam, releasing the water from an upstream reservoir, and an open-channel system. Solely based on mass conservation equation and conveyance considerations, the model could represent the three hydrograph types by adjusting the relative weight of each extreme configuration. Additionally, the dike vertical and lateral erosion evolutions were parametrized using three parameters. Among them, parameter *n* allowed us to characterize the dike strength, i.e. the larger the dike cross section, the stronger it is. Figure 5 presents non-dimensional breach hydrographs obtained with this model. For more information about the conceptual model, the reader may refer to Schmitz et al. (2021).

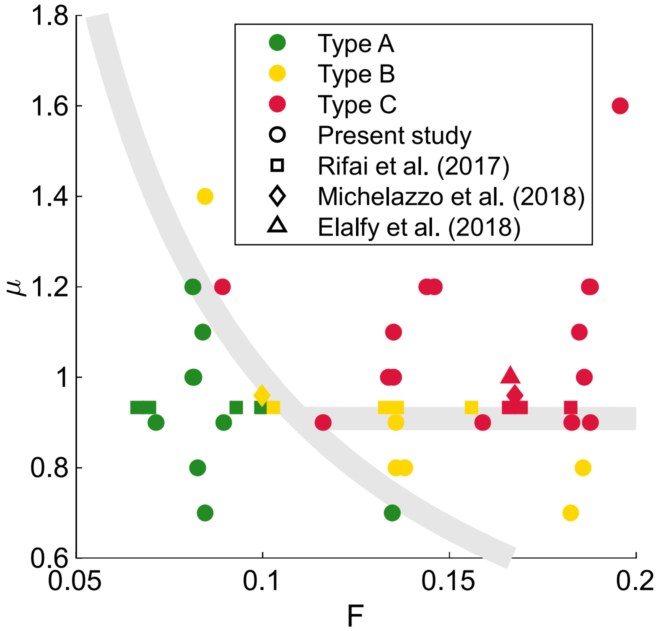

Figure 4. Occurrence of Types A, B and C breach hydrographs in the present study as well as in experimental tests conducted by Rifai et al. (2017), Michelazzo et al. (2018) and Elalfy et al. (2018) at laboratory scale. Grey-shaded lines represent transition zones.

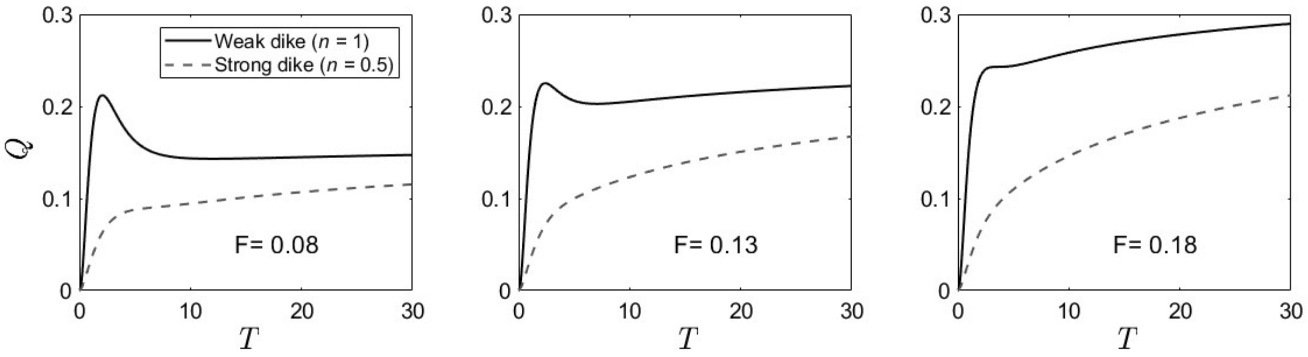

Figure 5. Non-dimensional breach hydrographs computed by the conceptual model for the three inflow discharges considered in the laboratory experiments.

4. CONCLUSIONS

This paper considered the breaching of laboratory-scale homogeneous non-cohesive fluvial dikes induced by overtopping and examined the influence of dike geometry on the breach hydrograph. The dike channel-side slope, floodplain-side slope and crest length were varied systematically. The normalized unit dike volume was found to capture successfully the overall effect of these parameters.

Based on eight dike configurations combined with three different inflow discharges, we observed that increasing the inflow discharge and enlarging the dike leads to a smoother increase in the breach discharge during Stage 1 and the more gradual transition between Stage 1 and Stage 2. Additional extreme configurations (i.e. dikes with particularly large and small cross sections) confirmed these observations. Also, three hydrograph patterns were identified. Their occurrence depends on the normalized unit dike volume and Froude number in the main channel.

Finally, a simplified conceptual model was implemented to demonstrate that a dike breach may be regarded as a combination of two idealized configurations, namely the breaching of a dam and an open-channel flow. Although the influence of several other parameters still needs to be investigated (e.g. main channel roughness, bottom erodibility, etc.), this work makes a valuable step forward in the understanding of the complex mechanisms underpinning dike breaching and the generated dataset might be used to validate numerical models.

5. REFERENCES

Elalfy, E., Tabrizi, A. A., & Chaudhry, M. H. (2018). Numerical and experimental modeling of levee breach including slumping failure of breach sides. *Journal of Hydraulic Engineering*, *144*(2), 04017066.

Michelazzo, G., Oumeraci, H., & Paris, E. (2018). New hypothesis for the final equilibrium stage of a river levee breach due to overflow. *Water Resources Research*, *54*(7), 4277-4293.

Müller, C., Frank, P. J., & Hager, W. H. (2016). Dyke overtopping: effects of shape and headwater elevation. *Journal of Hydraulic Research*, *54*(4), 410-422.

Rifai, I., Erpicum, S., Archambeau, P., Violeau, D., Pirotton, M., El Kadi Abderrezzak, K., & Dewals, B. (2017). Overtopping induced failure of noncohesive, homogeneous fluvial dikes. *Water Resources Research*, *53*(4), 3373-3386.

Rifai, I., El Kadi Abderrezzak, K., Erpicum, S., Archambeau, P., Violeau, D., Pirotton, M., & Dewals, B. (2018). Floodplain backwater effect on overtopping induced fluvial dike failure. *Water Resources Research*, 54(11), 9060-9073.

Schmitz, V., Erpicum, S., El kadi Abderrezzak, K., Rifai, I., Archambeau, P., Pirotton, M., & Dewals, B. (2021). Overtopping-Induced Failure of Non–Cohesive Homogeneous Fluvial Dikes: Effect of Dike Geometry on Breach Discharge and Widening. *Water Resources Research*, 57(7), e2021WR029660.